

CHEMISTRY AT THE GLASS TRANSITION: FLUORESCENCE-DETECTED PROTON
TRANSFER REACTIONS

A Thesis

by

KEEGAN WAYNE GRANFOR

BS, Texas A&M University-Corpus Christi, 2017

Submitted in Partial Fulfillment of the Requirements for the Degree of

MASTER OF SCIENCE

in

CHEMISTRY

Texas A&M University-Corpus Christi
Corpus Christi, Texas

May 2019

© Keegan Wayne Granfor

All Rights Reserved

May 2019

CHEMISTRY AT THE GLASS TRANSITION: FLUORESCENCE-DETECTED PROTON
TRANSFER REACTIONS

A Thesis

by

KEEGAN WAYNE GRANFOR

This thesis meets the standards for scope and quality of
Texas A&M University-Corpus Christi and is hereby approved.

Timothy P. Causgrove, PhD
Chair

Patrick Larkin, PhD
Committee Member

Hussain Abdulla, PhD
Committee Member

May 2019

ABSTRACT

Many liquids when cooled to cryogenic temperatures have the ability to take the form of a glassy substance; these are referred to as amorphous solids. As they are supercooled they do not form crystalline substances but rather an amorphous glass lacking in long-range structure. While the knowledge of these amorphous solids has been around for many years not much is known regarding the simplest physical and chemical processes that are allowed to occur within this glassy state. We introduce a new fluorescence-based temperature derivative spectroscopy methodology with the aim of discerning some of these physical and chemical attributes such as proton transfer in the glassy state.

Proton transfer in a cryogenic sample is accomplished by exploiting the photolytic capabilities of *o*-nitrobenzaldehyde. When exposed to ultraviolet light, *o*-nitrobenzaldehyde is transformed to *o*-nitrosobenzoic acid which has a relatively large acid dissociation constant. Fluorescein, a simple fluorescent molecule, and *o*-nitrobenzaldehyde were dissolved in a glycerol/water mixture and cryogenically supercooled below the glass transition temperature. The sample was then exposed to ultraviolet light and measured fluorometrically for alterations in the spectra. This experiment was repeated at varying viscosities and with deuterated solvents for measuring isotopic effects. The spectra were fit to first-order rate kinetic Arrhenius style equations to determine the energy barriers associated with the proton transfer.

Currently there is no documented use of temperature derivative spectroscopy using fluorometric based measurements to study dynamic processes and little if any information regarding simple chemical processes occurring within a supercooled glass sample. This research

provides a more detailed picture of these processes as well as describe a new methodology for temperature derivative spectroscopic experiments.

DEDICATION

I would like to dedicate this thesis to my wife, Brittany Nicole Granfor, who has been beside me through all of the ups and downs of this complicated time. I would also like to dedicate it to my grandparents, Karen and Larry Granfor, whom have helped support me throughout my entire academic career and life. Without you all I would not be where I am today.

ACKNOWLEDGEMENTS

I would like to thank my committee chair, Dr. Timothy P. Causgrove, and my committee members, Dr. Patrick Larkin and Dr. Hussain Abdulla, for their guidance and support throughout the course of this research.

Thanks also go to my friends and colleagues within the department of Physical and Environmental Science for making my time at Texas A&M University – Corpus Christi a pleasant experience. I particularly want to extend my gratitude to Mrs. Amber Maynard and Mr. Sebastian Rubanio, for continuously being there to understand and share in the tension that is research.

Finally, I want to thank the Instrument Coordinator, Mr. Nikolai Kraiouchkine, who trained me on the vast majority of analytical instrumentation found at Texas A&M University – Corpus Christi.

This research was financially supported by the National Science Foundation (NSF), Award #0616333, and by a departmental grant from the Welch Foundation, Award #634010.

TABLE OF CONTENTS

CONTENTS	PAGE
ABSTRACT.....	v
DEDICATION.....	vii
ACKNOWLEDGEMENTS.....	viii
TABLE OF CONTENTS.....	ix
LIST OF FIGURES	xi
LIST OF TABLES.....	xii
CHAPTER I – Introduction	1
1.1 Background Information	1
1.2 The Heavy Isotope Effect on the Kinetics of Energy Barriers.....	2
CHAPTER II – Literature Review.....	4
2.1 Glass Polymorphism	4
2.2 Proton Diffusion in Relation to the Glass Transition Temperature	4
2.3 Kinetic Isotope Effects.....	7
2.4 Kinetic Isotope Effects on Proton Motion.....	8
2.5 Variances in Glass Transition via Isotopic Exchange.....	10
2.6 Previous Experiments Using Photolytically Induced pH Jump Chemical Reactions ...	10
2.7 Previous Experiments Making Use of Temperature Derivative Spectroscopy (TDS)...	12
CHAPTER III – Research Goals	14
CHAPTER IV – Materials and Methods	15
4.1 <i>o</i> -Nitrobenzaldehyde Nomenclature and Photoionization	15
4.2 Sample Preparation	15

4.3	Fluorometric Evaluation.....	17
4.4	The Effect of Solvent Composition and Thermodynamic Extrapolation.....	18
CHAPTER V – Results.....		20
4.1	Fluorometric TDS Fitting Analysis.....	20
5.2	Isotopic Data Comparison.....	22
CHAPTER VI – Discussion		26
6.1	Overview	26
6.2	Variances in Old and New Glycerol	26
6.3	Observed Proton Transfer Step	27
6.4	Glass Transition on Proton Transfer	27
6.5	Abnormally High Observed Pre-exponential Values.....	28
6.6	Proposed Experiments.....	29
REFERENCES		30

LIST OF FIGURES

FIGURES	PAGE
Figure 1.1: Single well harmonic oscillator depiction of the difference in ZPE's of hydrogen and deuterium ions.....	3
Figure 2.1: Vehicle method of diffusion for a proton.....	5
Figure 2.2: Diagram of the Grotthuss Mechanism of proton transport.....	7
Figure 2.3: Semi-Classical (a) and Quantum Tunneling (b) double-well harmonic oscillator diagrams for crossing the PT energy barrier.....	9
Figure 4.1: Organic structures and pathway diagram for <i>o</i> NBA, the ketene intermediate, and deprotonated nitroso acid.....	15
Figure 5.1: 3-D representation of proton transport.....	20
Figure 5.2: Non-deuterated fluorescence data fit to Arrhenius style TDS equations.....	21
Figure 5.3: Deuterated fluorescence data fit to Arrhenius style TDS equations.....	22
Figure 5.4: Scatter plot of %Glycerol / %Glycerol[(OD) ₃] vs. T _{trans}	25

LIST OF TABLES

TABLES	PAGE
Table 5.1: Extrapolated glass transition information for the initial non-deuterated glycerol samples.....	23
Table 5.2: Extrapolated glass transition information from a new non-deuterated glycerol sample and the deuterated glycerol[(OD) ₃] samples.....	24

CHAPTER I – Introduction

1.1 Background Information

Since the mid 1800's chemists and physicists have been attempting to understand motion on a molecular level. Many theories have sprung up pertaining to molecular motion including classical mechanics, quantum mechanics and variations/syntheses of the two. Classical mechanics describes molecular motion for the simplest ion, hydrogen (H^+), as a set of steps involving fixed energy barriers (E_a) that the ion's kinetic energy must surpass to in order to transfer from one fixed location to another (i.e. proton transfer). It has since been observed that not all molecules follow the structure of classical mechanics and to a degree have the ability to bypass certain energy barriers via "tunneling" under them. This mechanism of tunneling was first observed by Henri Becquerel in 1896 and brought into the quantum mechanical theory in 1925 by Erwin Schrödinger and his associates. There have been variations of the two theories as some molecules only partially follow one theory, or follow only one theory under a certain set of conditions/parameters. To better understand the mechanisms pertaining to classical and quantum mechanics, as well as the thermodynamics and kinetics pertaining to proton transfer (PT) *o*-nitrobenzaldehyde (*o*NBA) was studied for its photochemical properties.

First described in 1980 by George and Scaiano¹ through UV/Vis measurements, when *o*NBA absorbs ultraviolet light it undergoes an intramolecular rearrangement which in turn can rapidly (on the order of nanoseconds) release a proton into solution. This elementary rearrangement and release of H^+ makes *o*NBA the ideal compound for irreversible acidification (i.e. pH jumps) of solutions, allowing pH dependent properties of a sample to be triggered remotely. Measuring alterations within the pH dependent properties of the sample allows for

determining thermodynamic and kinetic properties of the rearrangement and release of hydrogen ions.

1.2 The Heavy Isotope Effect on the Kinetics of Energy Barriers

For evaluation of the isotope effect, the solvent compounds were replaced with their deuterated counterparts. Preparing the sample in deuterated solvents will cause any exchangeable hydrogen to be replaced by the heavier isotope deuterium. Under normal room temperature conditions, the photolysis of *o*NBA results in the release of a hydrogen ion, which may attach to a vehicle molecule (e.g. water or deuterium oxide), and may diffuse through solution at the same rate as the vehicle molecule until reaching its final destination². A hydrogen ion under these normal room temperature conditions may also take part in the Grotthuss mechanism of molecular transport which relies on proton hopping through a hydrogen bonding network by formation/cleavage of the hydrogen bonds. Hydrogen ions found in non-diffusive environments, such as a cryogenically frozen glycerol/water glass samples, do not have the luxury of using a vehicle for transport as the solvent molecules are semi-frozen-in-place and must rely solely on the Grotthuss mechanism of molecular transport³⁻⁴. Due to the change in ion transport with varying environments, and the addition of the doubled mass of the hydrogen being replaced with deuterium allows for altered kinetics when encountering the PT energy barrier.

Different isotopes of the same element do not always have similar thermodynamic or kinetic properties. There are two methods of crossing the PT energy barrier: the classical “over barrier” method and the quantum mechanical “tunneling” method⁵. Classically speaking, due to the excess weight of the neutron for deuterium when comparing the rate constant (*k*) hydrogen can dissociate approximately 7x faster than deuterium. There is a drastic change in the rate of dissociation due to varying energy barrier heights between hydrogen and deuterium. This

difference manifests from the dissimilarity in masses of hydrogen and deuterium ions which results in a difference in the zero-point energies (ZPE) as portrayed below in Figure 1.1. In the PT for photo-ionization of *o*NBA this variance in energy barrier height leads to isotopic differences in rate of dissociation.

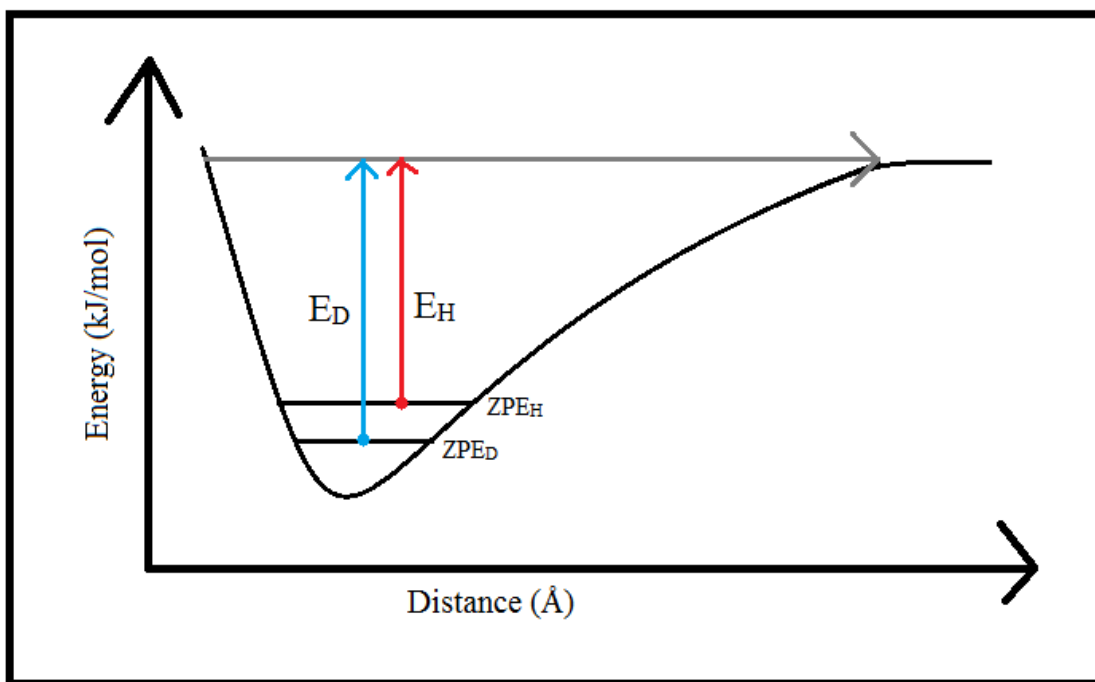


Figure 1.1. Single well harmonic oscillator depiction of the difference in ZPE's of hydrogen and deuterium ions.

The alternative method of crossing the energy barrier, quantum tunneling, is predicted to have different kinetic behavior when compared to its classical counterpart⁵. Quantum tunneling is a quantum mechanical phenomenon in which a molecule crosses a higher energy barrier (E_a) compared to its own internal energy. This occurs through alternate means not allowed by classical conservation of energy, meaning that the classical and quantum versions of the rate constants (k) would differ from each other.

CHAPTER II – Literature Review

2.1 Glass Polymorphism

Many combinations of liquids including, but not limited to, glycerol/water mixtures may form a glassy solid substance at cryogenic temperatures depending on the relative concentrations of the starting materials and the rate at which they are cooled⁶⁻⁷. The temperature at which thermal energy is reduced enough to transform the sample to glass is known as the glass transition temperature (T_g). Glass samples however may not be a true solid crystalline structure with uniformly arranged molecules but an amorphous solid with a randomly assembled structure. While in this glassy state molecules behave more similar to solids than liquids with translational diffusion “frozen out,” limiting molecular movement to atomic vibrations. If the temperature is raised above T_g the solidified structure is able to relax and molecular movement and diffusion may return to that of an average liquid. Below T_g the polymorphism of the glass sample is primarily driven by the solvent composition rather than the cooling rate, but the cooling rate may also play a vital role⁶. Definitionally, polymorphism is the ability to occur in a multitude of forms. As described in Bachler et al., glycerol/water mixtures with molar fractions of glycerol ranging from 0 to 0.38 are liable to form some amount of ice, while mixtures with molar fractions greater than 0.38 will not form any ice⁶.

2.2 Proton Diffusion in Relation to the Glass Transition Temperature

To fully understand a simple chemical reaction near T_g , one must understand molecular transport above and below the transition. Above T_g the sample is able to act as a fluid, and molecules can simply diffuse through solution. In the case of a proton, it may diffuse through the solution at the same rate as any molecule (e.g. water) it attaches to, known as the vehicle method of diffusion². The most simplistic example is that of water molecules which may form a covalent

bond with a proton and shuttle it to its final destination at the same rate of H₂O diffusion through the sample solution². Figure 2.1 portrays the ability of a proton to diffuse through solution via the vehicle mechanism. When taking up the proton, the water molecule transforms into the hydronium ion H₃O⁺ until releasing it at its destination, as the proton is extremely labile due to vast differences in the acid dissociation constants (K_a) of water and hydronium ion. The limiting step for PT is the vehicle's (i.e. hydronium ion) rate of diffusion².

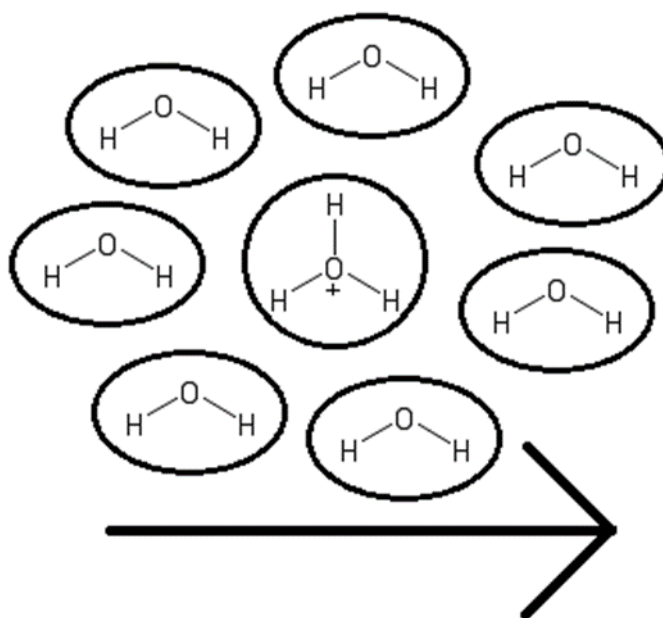


Figure 2.1. Vehicle method of diffusion where the proton is transported along with the parent hydronium ion at the same general rate of diffusion.

The rate of the vehicle method of diffusion may be suppressed through factors such as viscosity due to solvent composition or temperature. As temperature increases viscosity decreases, but solvent composition (i.e. a high concentration of glycerol to water) can also limit the rate of diffusion. As the viscosity decreases there is more freedom of molecular movement independent of how the viscosity is decreasing. A similar statement can be made about increasing solvent viscosity, whether due to temperature decreases in the sample or the with addition of a more

viscous solvent. In either case, molecular movement is vastly decreased until reaching a viscosity indistinguishable from that of a solid. When temperature is reduced to the point of T_g the vehicle diffusion mechanism is completely inhibited. Once viscosity has reached that of a solid, and/or the temperature has transversed below T_g the majority of molecular diffusion stops and only vibrational motion can occur. This leaves only the second type of PT through solution the Grotthuss mechanism³⁻⁴.

The Grotthuss mechanism describes the molecular transport of protons by a ‘hopping’ scenario through a hydrogen-bonded matrix³. Protons may use this mechanism while also taking part in vehicle diffusion, but they are solely limited to this type of molecular transport in a non-diffusive environment such as highly viscous solutions, or glass samples below T_g . The process is not tied to diffusion but rather the formation and cleavage of covalent bonds through the hydrogen bonding network one molecule at a time. Since it does not rely on the rate-limiting movement of molecular diffusion it has been identified as a mechanism for ultrafast PT in non-diffusive environments⁸⁻⁹. While this method is extremely fast compared to vehicle diffusion, it is important to keep in mind that the original proton shuttled may not end up being the same one that reaches the final destination. Figure 2.2 demonstrates the functionality and journey taken by a proton participating in the Grotthuss mechanism of transport. In the case of a hydronium ion the active proton may form a partial hydrogen bond with a neighboring water molecule. Once the partial bond is in place the proton may sever its original covalent bond with the hydronium ion and then solidify its partial hydrogen into a covalent bond with the receiving water molecule, which is observed as hopping from one molecule to the next. The proton may hop as frequently as the parent molecule can form bonds with other neighboring molecules, the larger the hydrogen bonding network the more effective the Grotthuss mechanism of transport. This is due to the bonds being

formed and cleaved in the most efficient manner possible and the most favorable hydrogen ion based on the relative location to the H^+ being transferred.

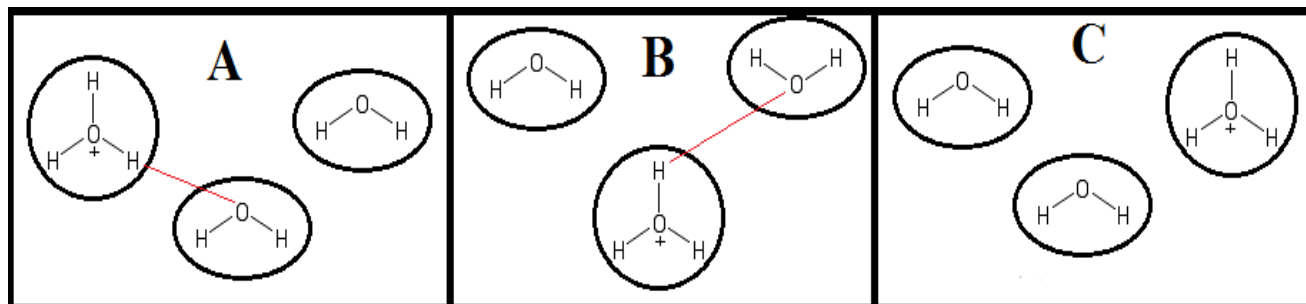


Figure 2.2. Diagram of the Grotthuss Mechanism of PT where the hydronium ion in block A forms a partial hydrogen bond (red line) with a neighboring water molecule and proceeds to “hop” to the neighboring molecule (B) until finally it reaches its final destination (C).

The deciding factor on how a proton will move through solution depends on the viscosity, composition, and temperature of the sample. As viscosity increases to near that of a solid, and as temperature decreases to near T_g , the Grotthuss mechanism is the exclusive method of transport, while at high temperature and low viscosity vehicle diffusion is able to occur in combination with the Grotthuss mechanism.

2.3 Kinetic Isotope Effects

Temperature, viscosity, and density are the main factors driving how protons are transferred through solution but it is also worthwhile noting how isotopic effects can alter PT at the glass transition. By exchanging all labile protons in the solvent matrix with their deuterated counterparts (e.g. deuterium oxide and glycerol[(OD)₃]) steps in the Grotthuss mechanism transfer D^+ rather than H^+ . The heavier mass can have varying effects on the kinetics observed in simple chemical reactions, but can also change the polymorphism of the glycerol/water glass. In this study, the third isotopic form of hydrogen, tritium, will not be discussed due to its instability and extremely small relative abundance¹⁰. Deuterium however is an interesting case as a stable isotope

and its additional neutron found in the nucleus when compared to hydrogen. As hydrogen is a simple proton with a relatively weightless electron, the increased mass of the neutron found in deuterium virtually doubles the mass of the ion, which is the largest isotopic change in mass (as a percentage) that is currently known. The large difference in isotopic masses fully augments the effects seen in the rate constants (k) when comparing the two isotopes (eq. 2.1).

$$\frac{k_H}{k_D} = k_{isotpoic\ distribution} \quad eq. 2.1$$

2.4 Kinetic Isotope Effects on Proton Motion

There are two theories of motion that are widely accepted: classical mechanics brought to light by Isaac Newton and the quantum mechanics illustrated by Erwin Schrödinger. In terms of molecular motion, a pure classical mechanic view is inappropriate, but not all molecules participate in quantum mechanical tunneling, leading to a synthesis of the two theories. Classical mechanical views were modeled through the general harmonic oscillator equation (eq. 2.2), which is inappropriate due to constant atomic vibrations. In this equation ν_o represents the oscillating frequency, k is the force constant, and m is the mass of the observed particle⁴.

$$\nu_o = \frac{1}{2\pi} \sqrt{\frac{k}{m}} \quad eq. 2.2$$

Ideally one must look at molecular motion in either a semi-classical or quantum mechanical view due to constant vibrations above zero Kelvin. Semi-classically one must consider the zero point energy (ZPE) for those molecules, and for PT to occur an activation energy (E_a) larger than the ZPE at any reactant or transition phase and that of the potential energy barrier must be brought about¹¹. ZPE itself is a quantum concept (which is the reason for deeming this motion semi-classical) that describes the lowest achievable ground state energy for a particular molecule. This

can be modeled by equation 2.3 where E_o and ν are the lowest possible energy ground state and the vibration oscillation for a particular molecule, and \hbar is Planck's constant divided by 2π .

$$E_o = \frac{1}{2} \hbar \nu \quad \text{eq. 2.3}$$

Since deuterium has double the mass of hydrogen the vibration frequency is drastically slower, implying the lowest possible ground state for hydrogen (E_o) is above that of deuterium meaning hydrogen has a greater transfer probability than deuterium. As the ground state energy increases the relative height of the energy barrier is reduced, reducing the activation energy required to cross. This semi-classical theory can best be modeled through a double-well harmonic oscillator as in Figure 2.3a.

Speaking semi-classically k_H/k_D ratios should be somewhere in the range of ~ 1 -10 but some observed ratios are considerably higher (see Melander and Saunders¹² for a summary of kinetic isotope ratios). These considerably high ratios are further elaborated upon by the second proposed theory of molecular motion: quantum tunneling^{11, 13-14}. Quantum tunneling is highly dependent on the isotopic mass of the molecule resulting in a very large kinetic isotope effect. While this has not been extensively examined in simplistic PT reactions near the glass transition, exceedingly large isotopic rate ratios are an indication of tunneling which is modeled in Figure 2.3b

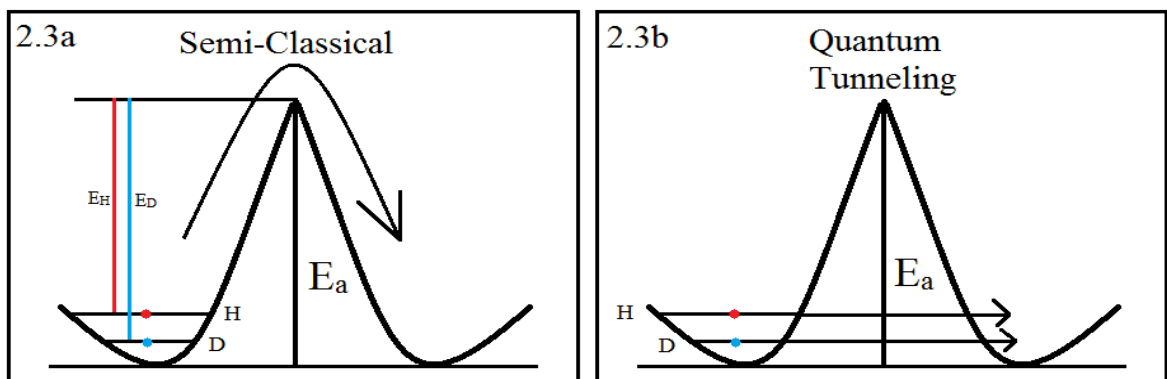


Figure 2.3. Semi-Classical (a) vs Quantum Tunneling (b) double well harmonic oscillator diagrams for crossing the PT energy barrier. E_a is the general activation energy for the entire barrier, E_H is the PT energy barrier for hydrogen and E_D is the PT energy barrier for deuterium.

2.5 Variances in Glass Transition via Isotopic Exchange

Isotopic effects can also be observed in the polymorphism of glass samples and the temperature at which T_g is found to occur. Since T_g is highly dependent on properties such as density, isotopes with varying densities (e.g. hydrogen and deuterium) can have altered glass transitions. An ideal model for observing this alteration is the difference in water and deuterium oxide glass transitions. While hydrogen or deuterium do not make up a large part of the mass of the two compounds, relatively speaking there is a large change in molecular weight when comparing the two as well as a change in density. Not many experiments have been performed to fully explain the glass transition of pure water or deuterium oxide for the simple fact that these substances prefer the formation of ice crystals to that of glass below 273K. While difficult to observe, supercooling and hyperquenching the solutions has led to the accepted value of T_g for pure water to be around 136K while the T_g for deuterium oxide is around 140K¹⁵⁻¹⁶. More recent experiments, making use of dielectric-spectroscopy figures of vapor-deposited amorphous water, have suggested the difference in T_g to be $10 \pm 2\text{K}$ ¹⁷. These temperature transitions may not be exact due to differences in sample preparation, cooling rate, and measurement techniques but there is clearly a measurable difference in the glass transition temperature of the two isotopes.

2.6 Previous Experiments Using Photolytically Induced pH Jump Chemical Reactions

Some early applications of *o*NBA as a photogenerated acid can be traced back to the 1990s and very early 2000s. In 1994 Hammes-Schiffer and Tully used *o*NBA to study the molecular dynamics of PT in solution⁵. In 1998 Carcelli et al. attempted to gather more data on the short-lived photolyzed ketene intermediate (Fig. 4.1) while that same year Gershenon et al. started some of the first true pH jump experiments¹⁸⁻¹⁹. In 2000 Abbruzzetti et al. began to study the kinetics of

helix formation in poly-L-glutamic acid which paved the way for many other photolytic research projects²⁰⁻²³. Shortly after in 2001 the Abbruzzetti group studied photoinduced alkaline pH jumps and the kinetics of histidine de-ligation from heme through laser-induced pH jumps²⁴.

The photolytic capabilities of *o*NBA are not limited to purely physico-chemical studies but can further expand into other scientific fields such as biochemistry. In 2003, Mallik et al. used laser induced pH jumps via *o*NBA to study the sub-millisecond protein dynamics and kinetics of excited state proton transfer (ESPT) in a mutant form of green fluorescent protein (GFP)²⁵. A photomultiplier tube and a 500 MHz oscilloscope were used to measure fluorescence intensity over a period of ~500 μ s. During that time the pH declined from 8 to 5 via laser photolysis of *o*NBA. The experiment was repeated with varying percentages of glycerol to test effects of viscosity during ESPT. This was supported by Kramers' Theory which describes how solvent dynamics will slow reaction rates, and showed that as the viscosity of the solvent increased kinetics of ESPT decreased²⁵. This implies that for 'large' molecules viscosity and protein dynamics for PT between solvent and fluorophore are intertwined²⁵.

Saxena et al. expanded on the work of Mallik et al. in 2005, using *o*NBA to further explain how viscosity and protein dynamics can affect ESPT in enhanced green fluorescent protein (EGFP)²⁶. Both papers concluded that solvent viscosity has an inverse relationship with the speed of ESPT, but the specifics of how viscosity provoked slower kinetics was not entirely determined in the Mallik paper, as they deduced two possible rate limiting steps. Saxena elaborated on the effects of viscosity by explaining how it could potentially reduce the transfer of protons from the protein-water interface to the fluorophore²⁶. The paper also discussed how reducing the PT from the protein-water interface is a more probable cause than that of viscosity slowing the ligand dissociation of the H-bond network for anionic B state stabilization²⁶. This is due to extreme

reductions in the EGFP ESPT rate constants when coupled with increasing viscosity, and that the ESPT through the interior of the protein is expected to be not, or at most, weakly coupled to solvent viscosity²⁶.

In 2012, Donten et al. expanded on a 2006 paper by Causgrove and Dyer which used photolytically generated pH jumps to study the α -helix folding of poly-L-glutamic acid^{21, 23}. This experiment was performed at room temperature with the use of *o*NBA photolytically generating H⁺ via a UV pulse pump at 266nm²¹. This experiment demonstrated the viability of pH jumps for future studies of peptide folding²¹.

More recently, Jeong et al. studied PT in the M2 proton channel of influenza virus A²⁷. The group used time-resolved tryptophan fluorescence, coupled with photolytically generated H⁺, to measure protein dynamics of the M2 proton channel transmembrane (M2TM) domain²⁷. They determined the protonation speed of histidine position 37 and observing the microenvironmental changes around tryptophan position 41 in M2TM when perturbed by pH alterations²⁷. This paper also describes the current use of pH jump fluorescence experiments and a variety of uses for the technique.

2.7 Previous Experiments Making Use of Temperature Derivative Spectroscopy (TDS)

In 1990 temperature derivative spectroscopy (TDS) was proposed by Berendzen et al. as a method for studying myoglobin protein dynamics as a complement to isothermal relaxation spectroscopy (IRS)²⁸. This was due to the limits posed by IRS in regards to the large separation of rates of certain measurable processes in a protein at a given temperature, while TDS can perform at a multitude of different temperatures²⁸. Since the TDS experiment time scales change as the sample is heated this allows for varying the time scales based on instrument parameters and

abilities as well as the molecular processes attempting to be observed²⁸. This in turn allows for the highly sensitive and extremely fast kinetic parameters to be observed on a slower, more favorable time scale²⁸. The paper also discussed their model for first-order kinetic rate processes that follow an Arrhenius temperature dependence. This was applied in our experiments and mathematics will be further elaborated upon in the materials and methods section²⁸.

Weik et al. (2004) used TDS with fluorometric measurements to study dynamic changes in single protein crystals soaked in fluorescein¹⁶. Depending on the location of the fluorescein (solvent or bound to the protein molecules) glass transition information as well as information concerning protein dynamics was obtained¹⁶.

While the idea of TDS experiments performed in tandem with a pH jump has not been extensively covered, one experiment has incorporated the use of TDS with the photolytic capabilities of *o*NBA. In 2013 Gregory et al. studied conformational changes in poly-L-glutamic acid by cryogenically lowering the thermal energy, below the helix-coil transition energy requirements, photolytically jumping the pH of the solution, and measuring for changes in the infrared spectrum²². This was an example how creating a non-equilibrium sample population via photolytically generated pH jumps would be a useful tool in a variety of future TDS experimental methods²².

CHAPTER III – Research Goals

*o*NBA is a well-known photolytic compound that, upon absorbing UV light, rearranges its molecular structure to become an acid and can therefore alter the pH of a solution. This elementary rearrangement allows the molecule to be used across many fields such as bio- and physical chemistry as an instant, irreversible acidification method within a sealed, isolated sample. The purpose of this research is to better understand how this method of acidification can be used in future experiments, to investigate cryogenic pH jump fluorometry, and determine what PT step is truly being observed (i.e. initial proton release by *o*NBA, proton transfer to/from solvent molecules, or final protonation of the fluorescein). It will engender further knowledge of the glass transition and PT energy barriers, along with the isotopic kinetic effects associated with those barriers.

CHAPTER IV – Materials and Methods

4.1 *o*-Nitrobenzaldehyde Nomenclature and Photoionization

o-Nitrobenzaldehyde (*o*NBA), or 2-nitrobenzaldehyde, was first described in 1980 by George and Scaiano¹. It was been widely used in the physico-/biochemical fields for its strong photo-acidification properties^{22, 25-26, 29}. When *o*NBA absorbs ultraviolet light, it undergoes an intramolecular rearrangement to *o*-nitrosobenzoic acid, or nitroso acid, which in turn can rapidly (on the order of nanoseconds) release a proton into solution^{1, 29}. During this rearrangement some molecules form a semi-stable ketene intermediate whose lifetime is dependent on solvent viscosity, while fully-formed nitroso acid molecules perform a back reaction leading to a 50% yield in hydrogen ion photolysis that is nearly independent of the solvent²⁹. This elementary rearrangement and release of hydrogen ions makes *o*NBA the ideal compound for almost immediate acidification of solutions to allow the study of pH-dependent properties^{1, 21-22, 25-27, 30}.

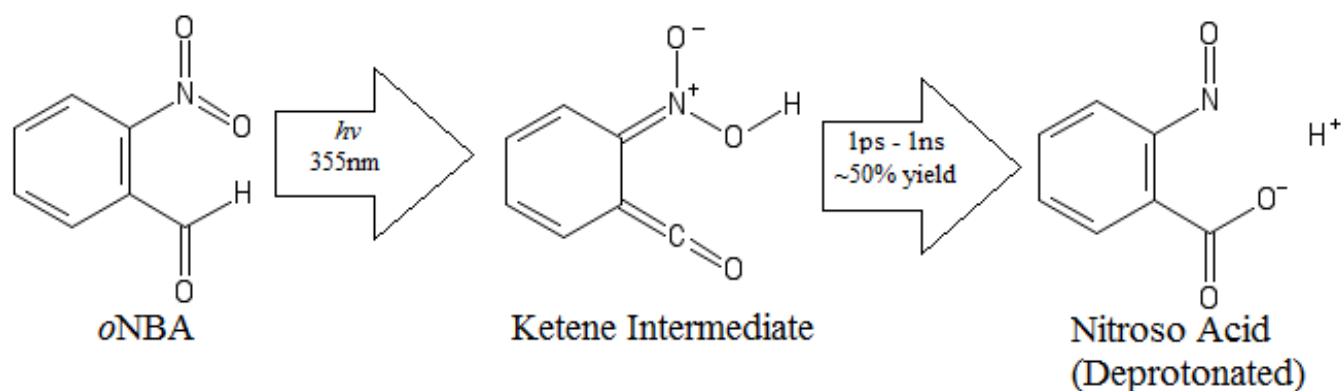


Figure 4.1. Organic structures of *o*NBA, the ketene intermediate, and deprotonated nitroso acid, along with a simple photolysis pathway diagram.

4.2 Sample Preparation

Non-deuterated samples were prepared using glycerol (99.5% anhydrous), water (filtered using a Biopak Polisher), *o*NBA (99%+), fluorescein sodium salt, and sodium hydroxide to ensure

basicity of the fluorescein. Deuterated samples were prepared with deuterated glycerol known as glycerol[(OD)₃] (98% anhydrous), deuterium oxide (99.9%), sodium deuterioxide (99.5% isotopic) in addition to *o*NBA and fluorescein. Both nondeuterated and deuterated samples were prepared at varying viscosities with glycerol/water and glycerol[(OD)₃]/deuterium oxide molar fractions ranging from 0.0889 to 0.7207.

A stock solution of *o*NBA was first prepared by dissolving solid *o*NBA in water (or deuterium oxide) up to its saturation point (~8 mM), while also preparing a 450 μM stock solution of fluorescein by dissolving fluorescein sodium salt in water (or deuterium oxide). The final solutions were prepared via mixing the stock solutions in the ratio of 1:1:18 fluorescein, *o*NBA and a glycerol/water (or glycerol[(OD)₃]/deuterium oxide) mixture respectively to achieve a specific viscosity. A small amount of each sample was taken and analyzed in UV/Vis using an 8452A diode array spectrophotometer (Hewlett Packard) before and after the addition of sodium hydroxide (or sodium deuterioxide) to ensure that fluorescein was fully deprotonated. From these final solutions 40 μL of sample was taken and encased between two sample windows formed from calcium fluoride and separated by a 100 μm polytetrafluoroethylene (PTFE) spacer. The calcium fluoride windows were then placed into a screw-threaded sample holder with indium wire wrapped around the base for adequate thermal conduction, it was then connected to an Oxford Instruments DN-V Opti-Stat cryostat for low temperature spectroscopic experiments. Cryogenic temperatures were then reached with the addition and controlled flow of liquid nitrogen through the cryostat. An Oxford Instruments ITC 503 Temperature Controller was attached to the cryostat which allowed for monitoring the sample temperature while also controlling temperature set points and accurately ramping the temperature over a set range.

Prepared samples were placed inside the cryostat and connected by a screw-threaded sample holder. A vacuum pump reduced the pressure around the sample to ~0.1 mPa. The low pressure insulated the sample and sublimated any ice formations within the cryostat during cryogenic temperatures. Liquid nitrogen was used to cool and anneal the sample, which allows for an even glass formation of the glycerol/water solvent over the range of temperatures covered⁶. The sample was first cooled at a rate of ~8K/min from 293K to 145K and allowed to sit at 145K for 1 minute. This was followed by an annealing step, which increased the temperature to 230K at ~8K/min and allowed to maintain that temperature for 15 minutes. Finally, the sample was cooled at ~8K/min to 150K and maintained for 1 minute.

4.3 Fluorometric Evaluation

Samples were then fluorometrically measured using a Fluorolog steady state and lifetime modular spectrometer (Horiba Scientific). Within the fluorometer, a 370 nm longpass filter and 500 nm shortpass filter (Edmund Optics) were attached in the excitation light optic pathway to ensure the removal of any light produced by the fluorometer that could photolyze the *o*NBA. A 500 nm dichroic long pass filter (Edmund Optics) was placed in the emission light optic pathway to reduce any possible scattering light effects close to the excitation wavelength (ex. 480nm). The temperature was then ramped at 1K/min over the temperature range of 150-220K. During the temperature ramp emission spectra were continuously recorded, exciting samples at 480nm and measuring fluorescence emission over the range 500-600 nm. Once the temperature reached 220K the ramp was stopped and designated “non-photolyzed,” which is a background reading of what the molecules do specifically with an increase in temperature but no pH change. The sample was cooled once again to 150K at ~8K/min. A Newport high power mercury-xenon lamp (MKS

Instruments) was then used to bombard the sample with high intensity UV light for 10 minutes. The absorption of this UV light by the sample allowed for the rearrangement of *o*NBA into the proton-labile nitroso acid^{1, 29}. The sample was then measured as before for fluorometric changes as the temperature increased at 1K/min from 150K to 220K. When enough thermal energy had been built to overcome the PT energy barrier a decrease in fluorescence occurred as protons flowed from the nitroso acid to the fluorescein molecules.

4.4 The Effect of Solvent Composition and Thermodynamic Extrapolation

Solvent composition in low temperature glycerol/water glass experiments can affect a variety of phenomena including glass transition temperature and ice pocket formations⁶. The role of solvent composition on the photolytic rearrangement and their release of hydrogen ions, and their movement was analyzed by comparing variations in the measurable parameters (activation energy, preexponential constant, and temperature of protonation) for different solvent viscosities. The samples had glycerol (or glycerol[(OD)₃]) molar fractions that ranged from 0.0889 to 0.7207 which were back-calculated from the refractive index of the solvent by an AR200 Automatic Digital Refractometer (AMETEK Ultra Precision Technologies). At cryogenic temperatures, molar fractions of glycerol greater than 0.38 form a transparent glass-like substance, while mixtures below 0.38 form an amorphous icy substance⁶.

Once the fluorometric data had been recorded (*Methods 4.2*) the dataset was graphed and analyzed using the Igor Pro (Wavemetrics) program. This program allows for fitting an energy barrier as a function of temperature from the fluorescent data using mathematical derivations of differential equations used for TDS by Berendzen et al.²⁸ (eq. 4.1).

$$\left[\frac{dN}{dT}\right] = -\left(\frac{Ni}{\beta}\right) ke^{-\theta} \quad \text{eq. 4.1}$$

Where N_i the initial population, β the heating rate, k the rate constant, and θ must be determined (eq. 4.2). θ is a mathematical relationship between the heating rate and rate constant described by Berendzen et al.²⁸.

$$\theta = \int_{T_i}^T \frac{k}{\beta} dT \quad \text{eq. 4.2}$$

The energy barrier information may then be extracted by fitting a fluorometric dataset with relation to the parameters of an Arrhenius equation using the Igor Pro (Wavemetrics) program and compared to other fluorometric datasets with varied viscosities. The Arrhenius equation relates the rate constant (k) to the pre-exponential constant (A), the activation energy (E_a), the temperature (T) and the ideal gas constant (R).

$$k = Ae^{\frac{-E_a}{RT}} \quad \text{eq 4.3}$$

These equations were used in tandem to yield information about the thermodynamic transitions of the photolytic release of hydrogen ion from photolyzed *o*NBA.

CHAPTER V – Results

A fluorescence-detected PT reaction in deuterated and non-deuterated solvents at the glass transition temperature is depicted in Figure 5.1. The figure presented below was formed from TDS data gathered after the parent *o*NBA molecules were exposed to UV light at 150K. The decrease in fluorescence is due to the PT at a specific temperature at all measured wavelengths.

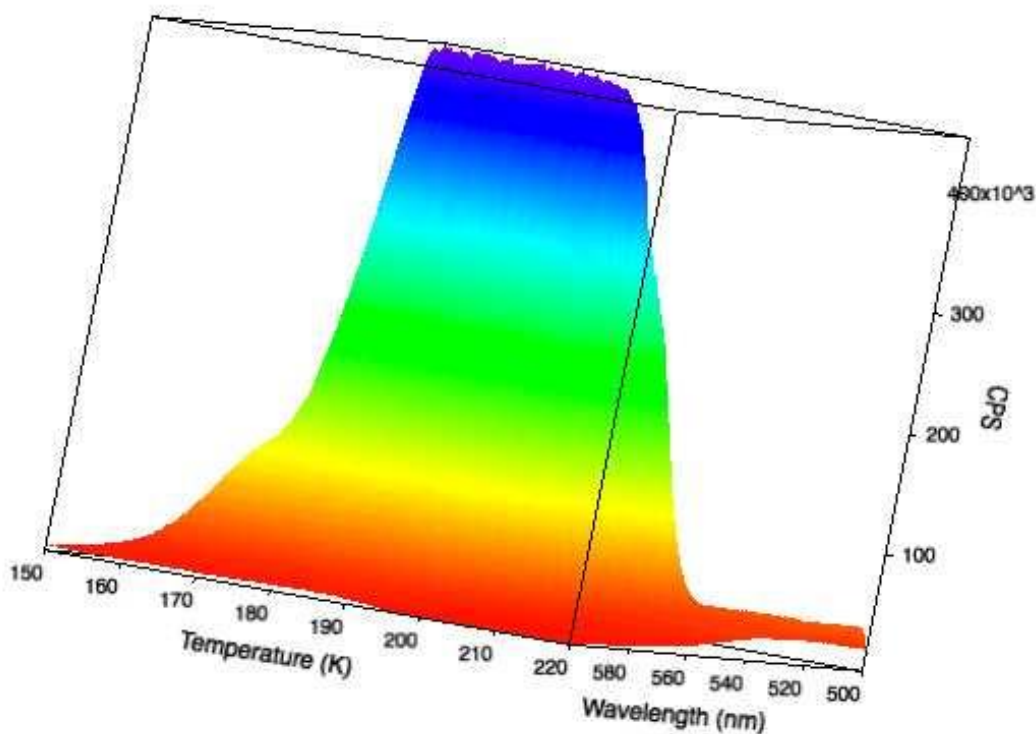


Figure 5.1. Fluorescence spectra from a 72.48% non-deuterated glycerol sample where PT is taking place. This 3-D representation is depicted by plotting the counts per second (CPS) as a function of both temperature and wavelength.

5.1 Fluorometric TDS Fitting Analysis

Figure 5.2 shows fluorescence data for a 72.48% glycerol sample with temperatures ranging from 150-220K. The spectra were averaged over 555-565 nm for the elimination of some noise in the data. The derivative of these spectra were then taken and fit to the mathematical

derivations of differential equations used for TDS by Berendzen et al.²⁸. The derivative dI/dT (counts/s/K), where I is fluorescence intensity, was plotted against temperature. The PT transition temperature (T_{trans}) is denoted by the peak (downward due to the decrease in fluorescence) in the graph.

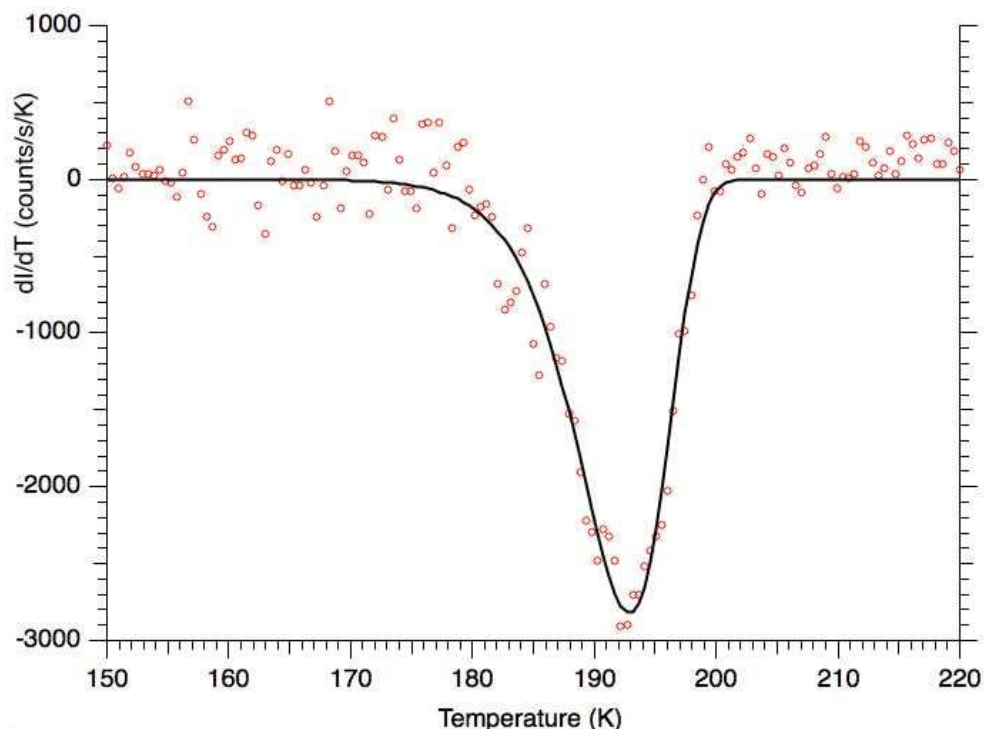


Figure 5.2. Fluorescence data for a 72.48% glycerol sample fit to Arrhenius style TDS equations depicting the PT reaction to occur at ~ 192 - 193 K.

Figure 5.3 shows fluorescence data for a 71.33% glycerol[(OD)₃] sample for temperatures ranging from 150-220K. The spectra were averaged over 510-520 nm for the elimination of some noise in the data. The change in fluorescence dI/dT (counts/s/K) was plotted against temperature. T_{trans} is again denoted by the peak in the graph.

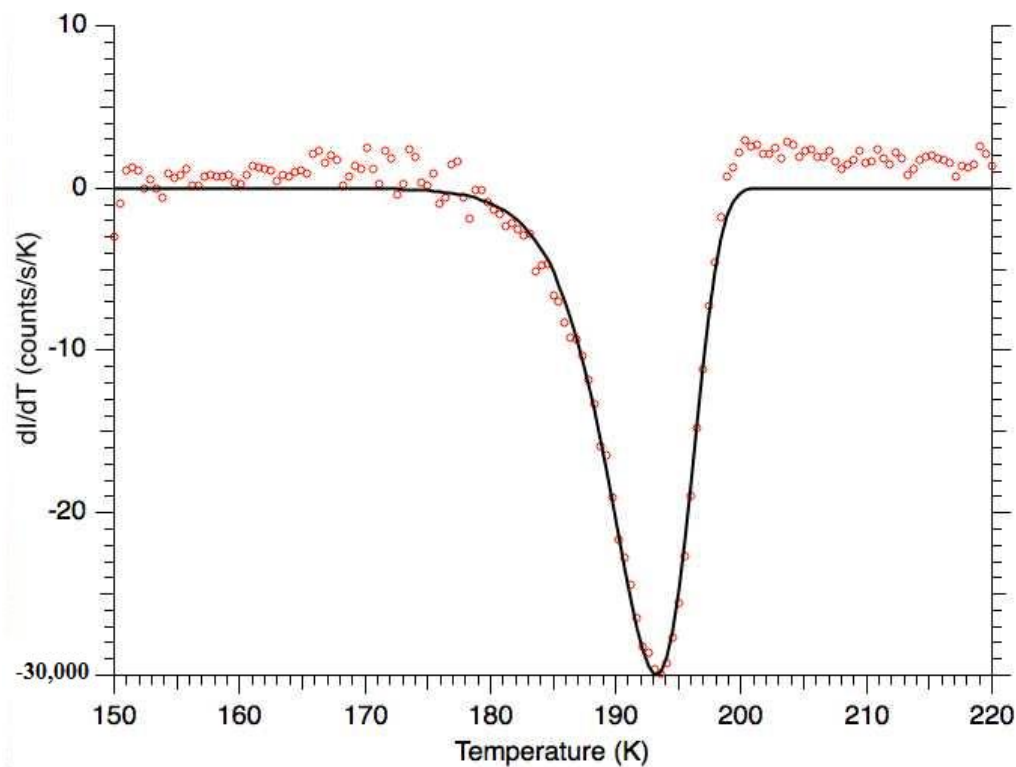


Figure 5.3. Fluorescence data for a deuterated 71.33% glycerol[(OD)₃] sample fit to Arrhenius style TDS equations depicting the PT reaction to occur at ~193K.

5.2 Isotopic Data Comparison

Non-deuterated and deuterated samples were prepared and analyzed from 28.36% glycerol (or glycerol[(OD)₃]) up to 90.81% glycerol (or glycerol[(OD)₃]). Light refraction analysis with an AR200 Automatic Digital Refractometer showed that the non-deuterated glycerol being used was not completely anhydrous before the dilution with water, so the initial non-deuterated samples analyzed were slightly below the target viscosity. This was not the case with the deuterated samples prepared with glycerol[(OD)₃]. This led to further analysis of the glycerol by UV/Vis spectroscopy. This showed the glycerol, before sample preparation, to have a slight absorption in the area of 275 nm, the region in which unphotolyzed *o*NBA absorbs. The data from these samples is displayed in Table 5.1. They initially displayed a variety of differences from their deuterated counterparts. The rate at 240K for both H⁺ and D⁺ were calculated from the pre-exponential

constant (A) and the enthalpy (H) parameters; this was chosen as an arbitrary reference point. The largest difference occurred between the 65.53% glycerol and the 63.14% glycerol[(OD)₃] (Table 5.2) samples which showed a ratio of rates (k_H/k_D) equal 4912.3. The smallest difference occurred between the 28.36% glycerol and the 30.86% glycerol[(OD)₃] (Table 5.2) samples being equal to 66.7.

%Glycerol	T _{trans} (K)	A (s ⁻¹)	H (kJ/mol)	Rate at 240K (s ⁻¹)	T _{glass} (K)
85.32%	189.1	2.30E+26	103.40	7.20E+03	186
72.91%	179.1	5.16E+25	95.60	8.00E+04	180
65.53%	172.5	1.50E+28	100.20	2.30E+06	174
56.31%	179.7	1.07E+25	93.80	4.10E+04	168
47.08%	179.7	1.10E+23	87.10	1.20E+04	163
38.07%	180.7	3.80E+23	89.30	1.40E+04	157
28.36%	180.7	1.09E+23	87.60	9.40E+03	152

Table 5.1. Initial information extrapolated for non-deuterated samples before changing the glycerol. T_{trans} represents the PT transition temperature (K), A is the preexponential constant (s⁻¹), H is the activation energy (kJ/mol), Rate at 240K is the PT rate at 240K (s⁻¹), and T_{glass} is the proposed glass transition temperature for that specific sample composition⁶.

After discovery of the small UV absorption in the 275 nm region, a second bottle of glycerol was purchased and analyzed via light refraction for its true viscosity and UV/Vis for any contaminants. It was verified to be completely anhydrous and did not absorb in at any wavelength from 230-700 nm. Some experiments were repeated to discern the validity of previous experiments performed with the original glycerol. A 72.48% sample prepared with the new glycerol was fluorometrically evaluated; results are displayed in Figure 5.2 and recorded in Table 5.2. Upon fitting the sample to Arrhenius style TDS equations it did not show any isotopic differences between its 71.33% deuterated counterpart. The ratio of rates at 240K between the two samples was equal to 0.178 displaying almost no difference in the PT between deuteration and non-deuteration of the samples. The information for both the new 72.48% glycerol sample and the

deuterated samples can be found in Table 5.2 along with the calculations of the kinetic isotope ratios.

Non-Deuterated					
%Glycerol	T_{trans} (K)	A (s^{-1})	H (kJ/mol)	Rate at 240K (s^{-1})	k_H/k_D
72.48%	192.7	8.40E+19	82.3	102.68	0.178
Deuterated					
%Glycerol[(OD)3]	T_{trans} (K)	A (s^{-1})	H (kJ/mol)	Rate at 240K (s^{-1})	k_H/k_D
90.18%	209.5	2.90E+20	91.5	3.53	-
80.58%	201.8	8.41E+22	97.6	48.08	-
71.33%	193.2	4.10E+23	95.8	577.70	0.178
63.14%	187.4	3.02E+20	81.8	474.30	-
53.32%	193.6	1.60E+18	76.4	37.63	-
41.88%	196.9	1.61E+20	85.2	46.01	-
30.86%	195.6	8.54E+21	90.9	140.24	-

Table 5.2. Information extrapolated from the new non-deuterated 72.48% glycerol sample and the deuterated samples 30.86% to 90.18%. T_{trans} represents the PT transition temperature (K), A is the preexponential constant (s^{-1}), H is the activation energy (kJ/mol), Rate at 240K is the PT rate at 240K (s^{-1}) and k_H/k_D is the ratio of rates.

Further visual depiction of the isotopic differences between the old and new glycerol, and the glycerol[(OD)3] is shown in Figure 5.4. This graph portrays how the old and new glycerol have vastly different PT temperatures. While this does bring up questions about the existence of an isotopic effect the data plot for old glycerol and glycerol[(OD)3] form similar curves with the lowest T_{trans} occurring at ~65% glycerol (or glycerol[(OD)3]), implying ~65% glycerol (or glycerol[(OD)]) is the most efficient place for PT to occur.

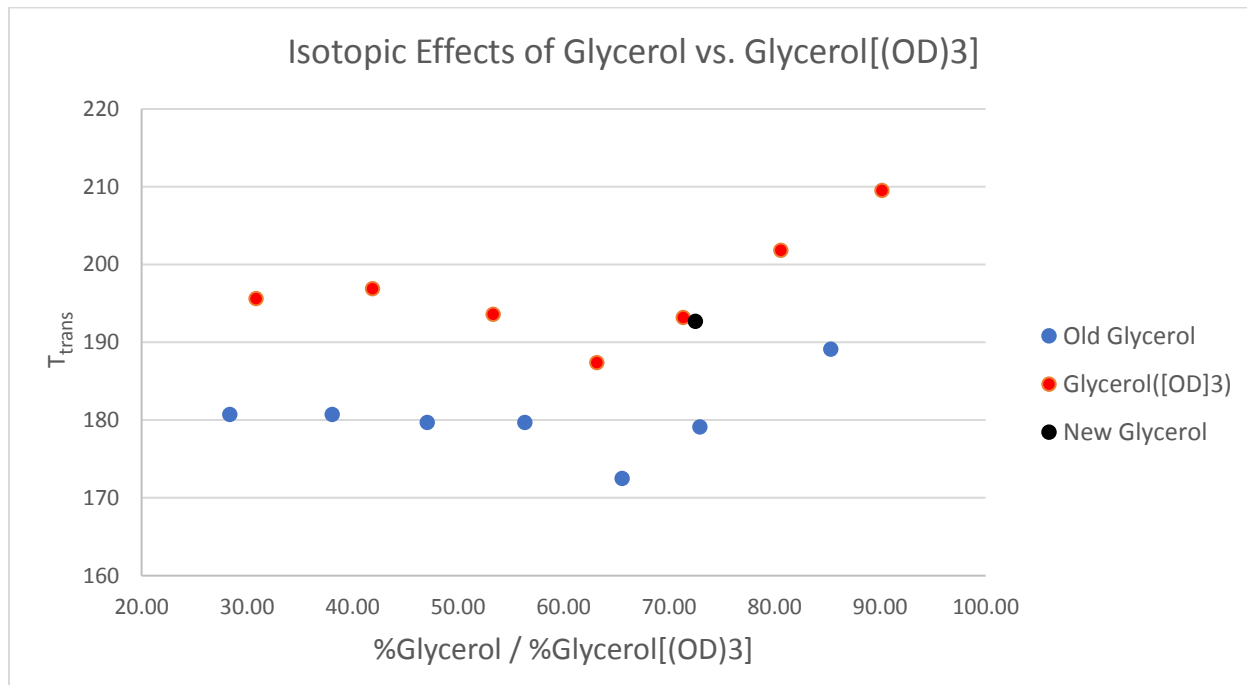


Figure 5.4. Plot of %Glycerol / %Glycerol[(OD)3] vs. T_{trans} that depicts the differences between the transition temperatures for the samples prepared with old vs. new glycerol. The old glycerol and glycerol[(OD)3] data points follow the same pattern with the lowest T_{trans} occurring at ~65%.

CHAPTER VI – Discussion

6.1 Overview

The experiments described here represent the first systematic direct observation of intermolecular PT dynamics at cryogenic temperatures. However, although PT is arguably the simplest possible chemical process, modeling the current experiments is surprisingly complex. Not only do questions of quantum tunneling vs. classical “over-the-barrier” mechanisms come into play, but models of classical mechanisms commonly depend on a reaction coordinate that includes solvent reorganization¹¹. At the glass transition, the structure of the solvent is not well characterized³¹. Recent experiments investigating solvents at the glass transition often measure bulk properties such as heat capacity or dielectric absorption³², making a complete view of solvent organization and its changes at the transition difficult. In contrast, PT specifically measures the relationship between well-defined donor sites and acceptor sites. Therefore, experiments such as the ones described here have the potential to yield much-needed information on the atomic-level dynamics occurring at the glass transition.

6.2 Variances in Old and New Glycerol

There were variances in the two non-deuterated glycerol samples available; one ‘old’ sample which had a small absorption in UV/Vis at ~275 nm, roughly in the same region as non-photolyzed *o*NBA, and one ‘new’ sample with no UV/Vis absorption at any wavelength from 230-700 nm. The absorption in the old glycerol led us to believe there was some contaminant, initially believed to be non-photolyzed *o*NBA or a combination of non-photolyzed and photolyzed *o*NBA. Further evaluation needs to be taken for discerning what the actual contaminant might be, but if it

is a different photolytic compound other than *o*NBA, a difference in transition temperatures would be reasonably expected.

6.3 Observed Proton Transfer Step

One of the research goals was to determine which PT step was actually being observed: H^+ leaving the parent *o*NBA molecule, H^+/D^+ being transported through the solvent, or H^+/D^+ attaching its self to the disodium fluorescein molecules. The observation of no isotopic differences when replacing all available solvent molecules with their deuterated counterparts implies that during photolysis the H^+ is not exchanged with the solvent, and that the observed step is that of H^+ leaving the parent *o*NBA compound. This conclusion is based on the hypothesis that the aldehyde hydrogen of *o*NBA is not labile during the formation and decay of the ketene intermediate (see Figure 4.1). If every labile hydrogen in the solvent and on the disodium fluorescein molecules is deuterated then the actual observed rate-limiting step is the initial release of hydrogen from the photolyzed *o*NBA.

6.4 Glass Transition on Proton Transfer

In the 2016 Bachler et al. paper the polymorphism of glycerol/water solutions are described⁶. According to their Figure 7, the melting temperatures of the glycerol/water samples have a similar shape as our plot of %Glycerol / %Glycerol[(OD)₃] vs. T but at much higher temperatures⁶. The temperature at which we observed PT to occur is much lower than the proposed melting temperature of glycerol/water so there is probably no correlation to that specific data⁶. Referring back to their figure 7, a combination of their proposed glass transition temperatures of molar fractions of (X_g) >0.3 (68.8% glycerol/glycerol[(OD)₃]) and proposed melting temperature

for icy domains form a pattern resembling our proposed PT temperatures in Figure 5.4⁶. From this correlation PT is proposed to occur at/near T_g for $X_g > 0.3$, and for $X_g < 0.3$ PT is proposed to occur at the melting temperature of the icy domains.

6.5 Abnormally High Observed Pre-exponential Values

Measured pre-exponential constant values for this experiment were much larger than the values predicted from transition state theory, which generally predicts values in the range of kT/h , or on the order of 10^{13} s^{-1} . Such values are consistently observed in hydrogen transfer experiments in solution³³.

The large pre-exponential constants are consistent with super-Arrhenius behavior, which is a phenomenon seen near the glass transition temperature in relaxation measurements such as volume expansion³⁴. This behavior is connected with the thermodynamics of the glass transition³⁵, and very recently a general, quantitative theory of super-Arrhenius behavior was published³⁶ that explains its connection with the thermodynamics of second-order phase transitions.

Also to be considered in the current experiments is that the photolytic compound is likely in a non-equilibrated state after the conformational change from *o*NBA to *o*-nitrosobenzoic acid. During the annealing step of the experiment the solvent molecules surrounding the photolytic compound should relax to their lowest conformational state. When the *o*NBA is exposed to high energy photons at 150K there is excess energy absorbed beyond the amount needed for the conformational change to *o*-nitrosobenzoic acid, which may result in the molecule and/or solvent molecules in non-equilibrated conformations. Upon reaching the glass transition temperature, the conformation starts to return back to that mirroring a liquid and where PT begins to occur. This

rapid conformational change and release of H^+ could potentially contribute to an extraordinarily high pre-exponential value.

6.6 Proposed Experiments

There are many future experiments that could be envisioned based on the results presented here. One obvious question is the exact origin of the differences in transition temperature seen in Fig. 4.4. If indeed this difference is due to the nature of the photolytic compound, then including a variety of photolytic compounds would explore various donor energy levels (changing the left-hand well of Fig. 2.3a). Therefore, substituting compounds such as: 2,4-dinitrobenzaldehyde, 2-nitro-4-(trifluoromethyl)-benzaldehyde, 2-chloro-6-nitrobenzaldehyde, 1-nitro-2-naphthaldehyde and 5-hydroxy-2-nitrobenzaldehyde would inherently provide more information about the PT in the glass / near-glass state. Based on the assumption that the aldehyde hydrogen is non-labile during photolysis, synthesis and use of deuterated *o*NBA would allow measurement of the kinetic isotope effect. Finally, one could use other glass-forming solvents with varying proton acceptor energies, changing the solvent reorganization coordinate. A comprehensive set of experiments addressing all of these variables would present the opportunity to thoroughly explore the atomic-level nature of the glass transition.

REFERENCES

1. George, M. V.; Scaiano, J. C., Photochemistry of o-nitrobenzaldehyde and related studies. *Journal of Physical Chemistry* **1980**, *84*, 492-495.
2. Kreuer, K.-D., Proton Conductivity: Materials and Applications. *Chemistry of Materials* **1996**, *8* (3), 610-641.
3. Tuckerman, M. E.; Chandra, A.; Marx, D., Structure and Dynamics of OH-(aq). *Accounts of Chemical Research* **2006**, *39* (2), 151-158.
4. Agmon, N., The Grotthuss mechanism. *Chemical Physics Letters* **1995**, *244* (5), 456-462.
5. Hammes-Schiffer, S. T., J. C., Proton transfer in solution: Molecular dynamics with quantum transitions. *The Journal of Chemical Physics* **1994**, *101* (6), 4657-4667.
6. Bachler, J.; Fuentes-Landete, V.; Jahn, D. A.; Wong, J.; Giovambattista, N.; Loerting, T., Glass polymorphism in glycerol-water mixtures: II. Experimental studies. *Phys Chem Chem Phys* **2016**, *18* (16), 11058-68.
7. Kauzmann, W., The Nature of the Glassy State and the Behavior of Liquids at Low Temperatures. *Chemical Reviews* **1948**, *43* (2), 219-256.
8. Vilčiauskas, L.; Tuckerman, M. E.; Bester, G.; Paddison, S. J.; Kreuer, K.-D., The mechanism of proton conduction in phosphoric acid. *Nature chemistry* **2012**, *4* (6), 461-466.
9. Ogawa, T.; Kamiguchi, K.; Tamaki, T.; Imai, H.; Yamaguchi, T., Differentiating Grotthuss Proton Conduction Mechanisms by Nuclear Magnetic Resonance Spectroscopic Analysis of Frozen Samples. *Analytical Chemistry* **2014**, *86* (19), 9362-9366.
10. Hutchison, S. G.; Hutchison, F. I., Radioactivity in Everyday Life. *Journal of Chemical Education* **1997**, *74* (5), 501.

11. Kiefer, P. M.; Hynes, J. T., Ultrafast Hydrogen Bonding Dynamics and Proton Transfer Processes in the Condensed Phase. In *Ultrafast Hydrogen Bonding Dynamics and Proton Transfer Processes in the Condensed Phase*, Elsaesser, T.; Bakker, H. J., Eds. Kluwer Academic Publishers: Dordrecht, The Netherlands, 2002; Vol. 23, pp 73-92.
12. Melander, L. C. S. S., William H., *Reaction rates of isotopic molecules*. Wiley: New York, 1980.
13. Nowick, A. S.; Vaysleyb, A. V., Isotope effect and proton hopping in high-temperature protonic conductors. *Solid State Ionics* **1997**, *97* (1), 17-26.
14. Bonanos, N.; Huijser, A.; Poulsen, F. W., H/D isotope effects in high temperature proton conductors. *Solid State Ionics* **2015**, *275*, 9-13.
15. Faizullin, M. Z.; Skokov, V. N.; Koverda, V. P., Glass transition and crystallization of water and aqueous solutions of organic liquids. *Journal of Non-Crystalline Solids* **2010**, *356* (23), 1153-1157.
16. Weik, M.; Vernede, X.; Royant, A.; Bourgeois, D., Temperature Derivative Fluorescence Spectroscopy as a Tool to Study Dynamical Changes in Protein Crystals. *Biophysical Journal* **2004**, *86* (5), 3176-3185.
17. Gainaru, C.; Agapov, A. L.; Fuentes-Landete, V.; Amann-Winkel, K.; Nelson, H.; Koster, K. W.; Kolesnikov, A. I.; Novikov, V. N.; Richert, R.; Bohmer, R.; Loerting, T.; Sokolov, A. P., Anomalously large isotope effect in the glass transition of water. **2014**, (1091-6490 (Electronic)).
18. Carcelli, M.; Pelagatti, P.; Viappiani, C., Determination of the pK(a) of the aci-nitro intermediate in o-nitrobenzyl systems. *Article* **1998**, *38* (3), 213-221.

19. Gershenson, A.; Fischer, C. J.; Schauerte, J. A.; Steel, D. G.; Gafni, A., Rapid events in protein folding studied by laser-induced pH and temperature jumps. *Proceedings of SPIE--the international society for optical engineering* **1998**, 3256, 252-262.
20. Abbruzzetti, S.; Viappiani, C.; Small, J. R.; Libertini, L. J.; Small, E. W., Kinetics of Local Helix Formation in Poly-L-Glutamic Acid Studied by Time-Resolved Photoacoustics: Neutralization Reactions of Carboxylates in Aqueous Solutions and Their Relevance to the Problem of Protein Folding. *Biophysical Journal* **2000**, 79, 2714-2721.
21. Donten, M.; Hamm, P., pH-Jump Induced α -Helix Folding of Poly-L-Glutamic Acid. *Chemical Physics* **2012**, in press.
22. Gregory, M. J.; Anderson, M.; Causgrove, T. P., Measurement of energy barriers to conformational change in poly-l-glutamic acid by temperature-derivative spectroscopy. *Chemical Physics* **2013**, 420, 1-6.
23. Causgrove, T. P.; Dyer, R. B., Nonequilibrium protein folding dynamics: laser-induced pH-jump studies of the helix-coil transition. *Chemical Physics* **2006**, 323 (1), 2-10.
24. Abbruzzetti, S.; Viappiani, C.; Small, J. R.; Libertini, L. J.; Small, E. W., Kinetics of histidine deligation from the heme in GuHCl-unfolded Fe(III) cytochrome c studied by a laser-induced pH-jump technique. *Journal of the American Chemical Society* **2001**, 123, 6649-6653.
25. Mallik, R.; Udgaonkar, J. B.; Krishnamoorthy, G., Kinetics of proton transfer in a green fluorescent protein: A laser-induced pH jump study. *0253-4134* **2003**, 4 (115), 307-317.
26. Saxena, A. M.; Udgaonkar, J. B.; Krishnamoorthy, G., Protein dynamics control proton transfer from bulk solvent to protein interior: A case study with a green fluorescent protein. *Protein Science* **2005**, 14 (7), 1787-1799.

27. Jeong, B. S.; Dyer, R. B., Proton Transport Mechanism of M2 Proton Channel Studied by Laser-Induced pH Jump. *J Am Chem Soc* **2017**, *139* (19), 6621-6628.
28. Berendzen, J.; Braunstein, D., Temperature-derivative spectroscopy: a tool for protein dynamics. *Proceedings of the National Academy of Sciences* **1990**, *87* (1), 1.
29. Donten, M. L.; Hamm, P.; VandeVondele, J., A Consistent Picture of the Proton Release Mechanism of oNBA in Water by Ultrafast Spectroscopy and Ab Initio Molecular Dynamics. *Journal of Physical Chemistry B* **2011**, *115* (5), 1075-1083.
30. Bizzarri, R.; Nifosì, R.; Abbruzzetti, S.; Rocchia, W.; Guidi, S.; Arosio, D.; Garau, G.; Campanini, B.; Grandi, E.; Ricci, F.; Viappiani, C.; Beltram, F., Green Fluorescent Protein Ground States: The Influence of a Second Protonation Site near the Chromophore. *Biochemistry* **2007**, *46* (18), 5494-5504.
31. Angell, C. A.; Ngai, K. L.; McKenna, G. B.; McMillan, P. F.; Martin, S. W., Relaxation in glassforming liquids and amorphous solids. *Journal of Applied Physics* **2000**, *88* (6), 3113-3157.
32. Wojnarowska, Z.; Tajber, L.; Paluch, M., Density Scaling in Ionic Glass Formers Controlled by Grotthuss Conduction. *J Phys Chem B* **2019**, *123* (5), 1156-1160.
33. Limbach, H. H.; Miguel Lopez, J.; Kohen, A., Arrhenius curves of hydrogen transfers: tunnel effects, isotope effects and effects of pre-equilibria. *Philos Trans R Soc Lond B Biol Sci* **2006**, *361* (1472), 1399-415.
34. Goldstein, M., On the Temperature Dependence of Cooperative Relaxation Properties in Glass-Forming Liquids—Comment on a Paper by Adam and Gibbs. *The Journal of Chemical Physics* **1965**, *43* (5), 1852-1853.

35. Cangialosi, D.; Alegría, A.; Colmenero, J., Relationship between dynamics and thermodynamics in glass-forming polymers. *Europhysics Letters (EPL)* **2005**, *70* (5), 614-620.
36. Medvedev, G. A.; Caruthers, J. M., A Quantitative Model of Super-Arrhenian Behavior in Glass-Forming Polymers. *Macromolecules* **2019**, *52* (4), 1424-1439.